© 2015. Published by The Company of Biologists Ltd | The Journal of Experimental Biology (2015) 218, 1621-1631 doi:10.1242/jeb.120444

RESEARCH ARTICLE

Mechanisms and costs of mitochondrial thermal acclimation in a eurythermal killifish (*Fundulus heteroclitus*)

Dillon J. Chung* and Patricia M. Schulte

ABSTRACT

Processes acting at the level of the mitochondria have been suggested to affect the thermal limits of organisms. To determine whether changes in mitochondrial properties could underlie shifts in thermal limits, we examined how mitochondrial properties are affected by thermal acclimation in the eurythermal killifish, *Fundulus heteroclitus* – a species with substantial plasticity in whole-organism thermal limits. We hypothesized that thermal acclimation would result in functional changes in the mitochondria that could result in trade-offs in function during acute thermal shifts. We measured the mitochondrial respiration rate ($\dot{V}_{O_2}$) through multiple complexes of the electron transport system following thermal acclimation (to 5, 15, 33°C) and assessed maintenance of mitochondrial membrane potential (Δp) and rates of reactive oxygen species (ROS) production as an estimate of costs. Acclimation to 5°C resulted in a modest compensation of mitochondrial respiration at low temperatures, but these mitochondria were able to maintain Δp with acute exposure to high temperatures, and ROS production did not differ between acclimation groups, suggesting that these increases in mitochondrial capacity do not alter mitochondrial thermal sensitivity. Acclimation to 33°C suppressed mitochondrial respiration as a result of effects on NADH dehydrogenase (complex I). These high-temperature acclimated fish nonetheless maintained levels of Δp and ROS production similar to those of the other acclimation groups. This work demonstrates that killifish mitochondria can successfully acclimate to a wide range of temperatures without incurring major functional trade-offs during acute thermal shifts and that high-temperature acclimation results in a suppression of metabolism, consistent with patterns observed at the organismal level.

KEY WORDS: Mitochondria, Thermal acclimation, ROS, Proton leak kinetics, Killifish, Ectotherm

INTRODUCTION

Environmental temperature imposes clear limitations on the geographic distribution of ectotherms because of the effects of temperature on the rates of biochemical reactions (Hochachka and Somero, 2002), which constrains whole-animal aerobic performance at thermal extremes. Indeed, aerobic scope (the difference between maximum and resting metabolic rate) has been demonstrated to decrease at the edge of species' thermal ranges (Eliason et al., 2011; Healy and Schulte, 2012; Pörtner and Farrell, 2008) implicating aerobic metabolism in establishing thermal limits. Improving understanding of the physiological and biochemical mechanisms that link temperature changes, aerobic scope, and organismal thermal performance is thus critical to providing predictive power over species' responses to global climate change.

Thermal performance curves of aerobic metabolism, a temperature-sensitive process that is crucial for maintaining eukaryotic energetic balance, can shift following thermal acclimation (Angilletta, 2009; Schulte et al., 2011). Although thermal acclimation may improve performance at the acclimation temperature, it can also cause a decrease in performance at temperatures that were not stressful prior to acclimation (e.g. a decrease in aerobic capacity at high temperatures following low-temperature acclimation). Changes such as these represent a 'cost of acclimation'. Identifying mechanisms that underlie these costs may provide insights into the factors that influence whole-animal thermal tolerance.

Due to its role in aerobic metabolism and energy balance, mitochondria are a likely site of processes influencing whole-organism thermal limits (Iftikar and Hickey, 2013; Pörtner, 2001), and thermal acclimation has been shown to alter mitochondrial properties in ways that may help to maintain aerobic scope. For example, previous studies have demonstrated low-temperature acclimation effects on mitochondrial enzyme function (Fangue et al., 2009; Kraffe et al., 2007), inner mitochondrial membrane (IMM) composition (for review see: Guderley, 2004; Grim et al., 2010; Kraffe et al., 2007), and mitochondrial volume density (Dhillon and Schulte, 2011; Egginton and Johnston, 1984; for review see: O'Brien, 2011). Although beneficial at the acclimation temperature, changes in mitochondrial physiology associated with thermal acclimation may result in dysfunction during acute thermal shifts (to previously unstressful temperatures), which may be a potential mechanism underlying shifts in thermal limits. For example, increased inner mitochondrial membrane fluidity during low temperature acclimation is thought to help maintain mitochondrial output at low temperatures by increasing the frequency of enzyme interactions and substrate diffusion rates (Hazel, 1995). An acute increase in temperature under these conditions, however, may result in membrane destabilization and a loss of the driving force to synthesize ATP (proton motive force, Δp; comprising a mitochondrial membrane potential, $\Delta\Psi_m$, and $[H^+]$ gradient). These effects represent a cost of low-temperature acclimation.

Acute high-temperature shifts, in contrast, are thought to increase mitochondrial function, resulting in deleterious consequences such as unsustainable O_2 consumption, and increased production of reactive oxygen species (ROS) (Abele et al., 2002). Acclimation to high temperatures therefore ought to result in a suppression of mitochondrial function to limit these effects. Thus, suppression of metabolism with acclimation to high temperature could be interpreted as a benefit of acclimation. Although there are relatively few studies examining this phenomenon, some groups have demonstrated that high-temperature acclimation results in a decrease in mitochondrial membrane fatty acid saturation and a decrease in respiration rate (Guderley and Johnston, 1996; Khan et al., 2014; Strobel et al., 2013).

Department of Zoology, University of British Columbia, 6270 University Blvd, Vancouver, British Columbia, Canada V6T 1Z4.

*Author for correspondence (dchungch@zoology.ubc.ca)

Received 3 February 2015; Accepted 23 March 2015

The Journal of Experimental Biology (2015) 218, 1621-1631 doi:10.1242/jeb.120444

List of symbols and abbreviations

a	temperature-dependent coefficient
CCP	carbonyl cyanide-4-(trifluoromethoxy) phenylhydrazone
CT_{max}	critical thermal maximum
CT_{min}	critical thermal minimum
DMSO	dimethyl sulfoxide
EGTA	ethylene glycol tetraacetic acid
ETS	electron transport system
FRL	free radical leak
IMM	inner mitochondrial membrane
k	rate constant
K	partition coefficient
OCLTT	oxygen and capacity limited thermal tolerance hypothesis
PDH	pyruvate dehydrogenase
Q_{10}	temperature coefficient
R	universal gas constant
RCR	respiratory control ratio
ROS	reactive oxygen species
T_a	ambient temperature
$T_{acclimation}$	acclimation temperature
T_{assay}	assay temperature
TPP^+	tetraphenylphosphonium ion
v_{ext}	volume outside mitochondria
v_{mt}	mitochondrial matrix volume
$\dot{V}_{H_2O_2}$	rate of H_2O_2 production (ROS production rate)
$\dot{V}_{O_2}$	respiration rate
Δp	proton motive force
$\Delta\Psi_m$	mitochondrial membrane potential

Eurythermal ectotherms are ideal models in which to test the role of the mitochondria in thermal acclimation because their broad thermal tolerance likely occurs through recruitment of detectable changes in physiology (Guderley and St. Pierre, 2002). Indeed, studies of mitochondrial thermal acclimation that focus on climate change often use stenothermal species, making eurythermal responses a crucial point of comparison. The Atlantic killifish (*Fundulus heteroclitus*) typifies this eurythermal physiology. These fish can be acclimated to temperatures from ~2°C up to ~35°C and can tolerate an even wider thermal range in acute challenges (with critical thermal temperatures: CT_{min}, −1°C and CT_{max}, 41°C). Their acute thermal limits are also highly plastic, shifting by more than 10°C when these fish are acclimated to different temperatures (Fangue et al., 2006). There are some data to suggest that warm acclimation (25°C) of *F. heteroclitus* may be associated with a trade-off in mitochondrial function because liver mitochondrial respiration from warm-acclimated groups is sustained at high T_{assay} (up to 37°C), but is significantly depressed compared with lower $T_{acclimation}$ groups (5 and 15°C) when assayed at low temperatures (5°C; Fangue et al., 2009). Similarly, low-temperature (5°C) acclimation also causes an apparent trade-off because respiratory control ratios (RCRs, an approximation of mitochondrial coupling) in low-temperature acclimated fish decline at high T_{assay} (37°C), precluding assessment of mitochondrial respiration (Fangue et al., 2009). What remains unclear from these data is the specificity of the changes, because mitochondria were only provided with an electron transport system (ETS) complex I-linked substrate (pyruvate), whereas work in goldfish (*Carrassius auratus*), indicates that thermal acclimation responses may be recruited through other ETS components, such as complex II (Dos Santos et al., 2013). In addition, the effects of acclimation on mitochondrial membrane potential and ROS production have not been assessed in *F. heteroclitus*, and thus the mechanisms underlying this apparent trade-off remain unknown.

In this study, we assessed the effects of thermal acclimation on respiration of *F. heteroclitus* liver mitochondria, maintenance of $\Delta\Psi_m$, kinetics of proton leak and ROS production when respiration is fuelled with different substrates. We addressed the following objectives: (1) to assess the degree to which thermal acclimation (4 weeks at 5, 15, and 33°C) alters mitochondrial capacity; (2) to determine whether these modifications are specific to individual components of the mitochondrial apparatus (i.e. pyruvate dehydrogenase, ETS complex I, and complex II); and (3) to determine whether these changes in capacity incur a trade-off that causes costs to function during acute thermal shifts (i.e. loss of Δp, and increased ROS production rate). In so doing, we provide an assessment of the role of mitochondria in the maintenance of whole-animal thermal performance and shifts in thermal tolerance following acclimation.

RESULTS

Whole-animal characteristics

Acclimation to 33°C resulted in a reduction of all measured whole-animal characteristics, when compared with both 5 and 15°C acclimations. Whole-animal mass was greater for both the 5°C (6.29±0.29 g) and 15°C acclimation (6.13±0.24 g) groups when compared with the 33°C (5.04±0.19 g) group (one-way ANOVA, $P_{acclimation}<0.0001$, N=103–105). A slightly different pattern was observed with wet liver mass (one-way ANOVA, $P_{acclimation}<0.0001$, N=103–105) where 15°C acclimation (0.26±0.01 g) resulted in a marginally greater mass than the 5°C acclimation (0.22±0.01 g) which was double that observed in the 33°C group (0.14±0.01 g). A similar pattern was observed for pooled liver mitochondrial protein concentration (suspended in 800 µl buffer, one-way ANOVA, $P_{acclimation}<0.0001$, N=14–15). Again, both the 5°C (13.07±1.25 mg ml^{-1}) and 15°C (13.12±0.98 mg ml^{-1}) acclimation groups had greater protein concentration when compared with the 33°C (7.00±0.71 mg ml^{-1}) acclimation.

Mitochondrial respiration rate and membrane potential (ETS complexes I and II)

We assessed the effect of thermal acclimation and acute changes in assay temperature on liver mitochondrial respiration rate and mitochondrial membrane potential fuelled through ETS complex I and complex II. Increased assay temperature resulted in an increase in glutamate+malate-fuelled (ETS complex I) state 3 (ADP-phosphorylating) respiration rate ($\dot{V}_{O_2}$; Fig. 1A; linear mixed-effect model, $P_{assay}<0.0001$) and there was a significant effect of acclimation temperature on respiration (linear mixed-effect model, $P_{acclimation}<0.0001$); however, there was also a significant interaction between acclimation group and assay temperature (linear mixed-effect model, $P_{interaction}=0.0231$). Following acclimation to 33°C, liver mitochondrial respiration in the presence of glutamate+malate decreased up to 75% (T_{assay}=5–37°C) when compared with mitochondria from fish acclimated to either 5 or 15°C and the effects of acute temperature shift were also less pronounced in mitochondria from the 33°C acclimated group.

As was the case for flux through ETS complex I, increases in assay temperature increased succinate-fuelled (complex II) state 3 respiration for all acclimation groups (Fig. 1B; linear mixed-effect model, $P_{assay}<0.0001$). Again, significant interaction and acclimation effects were detected (linear mixed-effect model, $P_{interaction}=0.035$, $P_{acclimation}\leq0.0001$). Acclimation to 33°C resulted in lower respiration rates at acute temperature shifts from 5 to 37°C; however, this reduction (up to 40%) was only detected in *post hoc* tests when compared with fish acclimated to 5°C.

Acclimation effects on succinate-fuelled state 4 (non ADP-phosphorylating) respiration rates differed from those measured under state 3 conditions (Fig. 1C). Increasing assay temperature

The Journal of Experimental Biology (2015) 218, 1621-1631 doi:10.1242/jeb.120444

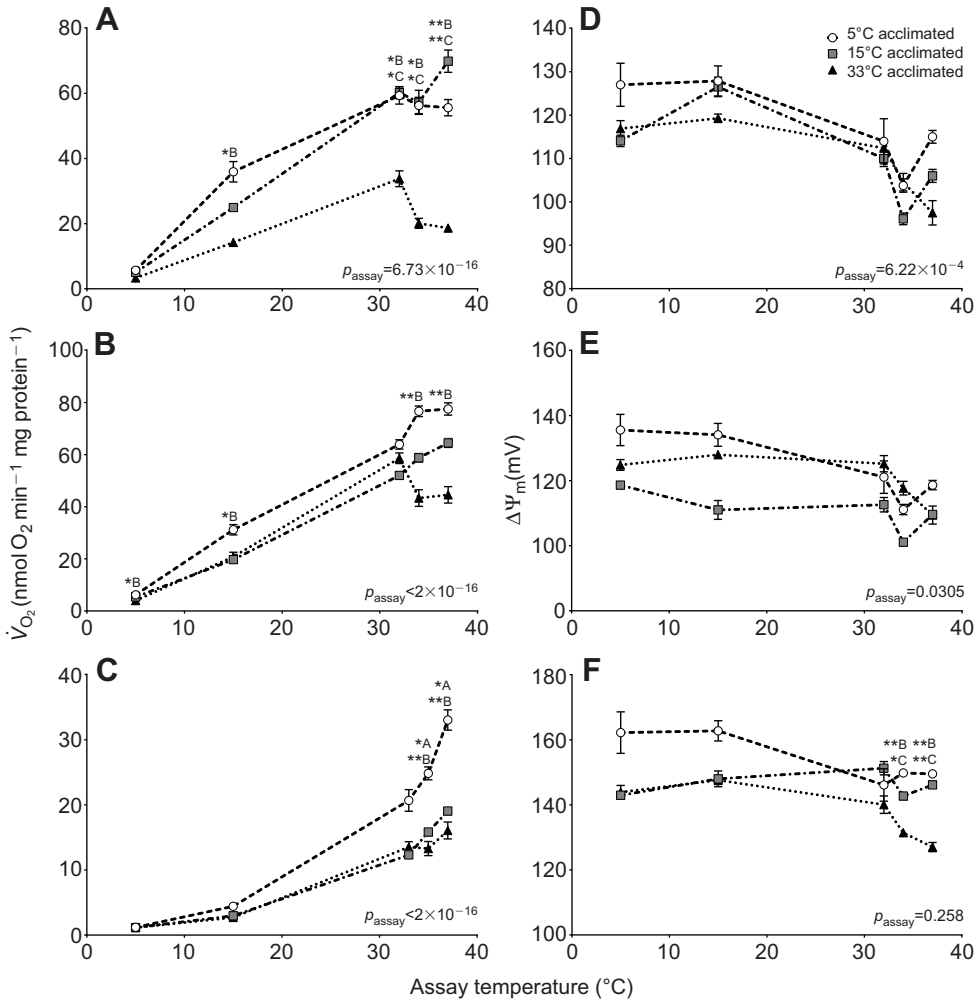

Fig. 1. Effects of acclimation and assay temperature on respiration rate and maximum membrane potential of liver mitochondria in the killifish *Fundulus heteroclitus*. Killifish were acclimated to 5, 15 or 33°C and mitochondrial parameters were measured in tandem over a range of assay temperatures. Mitochondria were provided complex I (A,D; glutamate+malate)- or complex II (B,C,E,F; succinate)-linked substrates and respiration rate was measured under state 3 (A,B,D,E) or state 4 (C,F) conditions. Assay temperature effects are indicated by *P*-value within each panel. Letters above each assay temperature indicate a significant difference between acclimations within an assay temperature (A, 5°C≠15°C; B, 5°C≠33°C; C, 15°C≠33°C). Asterisks denote the *P*-value of each acclimation effect (*P<0.05, **P<0.01). Data are means±s.e.m. (N=8–9).

increased succinate-fuelled leak respiration (linear mixed-effect model, P_{assay}<0.0001). Similar to succinate-fuelled state 3 respiration, both interaction and acclimation effects were statistically significant (linear mixed-effect model, $P_{interaction}$=0.0258, $P_{acclimation}$<0.0001). In this case, acclimation to 5°C resulted in higher leak respiration rates (T_{assay}=35 and 37°C) when compared with both 15 and 33°C acclimation groups.

To determine whether thermally acclimated mitochondria are able to maintain Δp (measured as $\Delta\Psi_m$, see Materials and methods for rationale) following acute thermal shifts (potentially representing a cost of acclimation), we measured $\Delta\Psi_m$ in tandem with previously described respiration rates (Fig. 1D–F). Acute increases in temperature significantly decreased mitochondrial membrane potential when respiring maximally (state 3) fuelled either through complex I (Fig. 1D; linear mixed-effect model, P_{assay}=6.22×10^{-4}) or complex II (Fig. 1E; linear mixed-effect model, P_{assay}=0.0305), but not during leak respiration fuelled through complex II (Fig. 1F; state 4). There was a significant effect of acclimation on membrane potential, but only for succinate-fuelled respiration measured under state 3 and 4 conditions (Fig. 1E,F; linear mixed-effect model, $P_{acclimation,state3}$=0.0092; $P_{acclimation,state4}$=0.0075). *Post hoc* analyses revealed that acclimation to 33°C decreased membrane potential, but only under maximum leak conditions (i.e. succinate-fuelled state 4) measured at high assay temperatures (T_{assay}=35 and 37°C). No additional significant main effects or interactions were detected.

Complex I- and pyruvate dehydrogenase-linked state 3 and 4 mitochondrial respiration

It is possible that the observed suppression of ETS complex I mitochondrial respiration could be dependent on the source of electrons (e.g. flux initiated by substrates entering the tricarboxylic acid cycle at different points). To assess this possibility, we measured state 3 and 4 respiration rates fuelled by glutamate and compared them with respiration rates fuelled with pyruvate (with malate to support the tricarboxylic acid cycle in each case). Glutamate enters the mitochondrion in exchange for aspartate and is converted by glutamate dehydrogenase into α-ketoglutarate for entry into the tricarboxylic acid cycle, whereas pyruvate enters the mitochondrion via a monocarboxylate transporter and is converted by the pyruvate dehydrogenase complex to acetyl CoA prior to entry into the tricarboxylic acid cycle (Halestrap, 2012).

The Journal of Experimental Biology (2015) 218, 1621-1631 doi:10.1242/jeb.120444

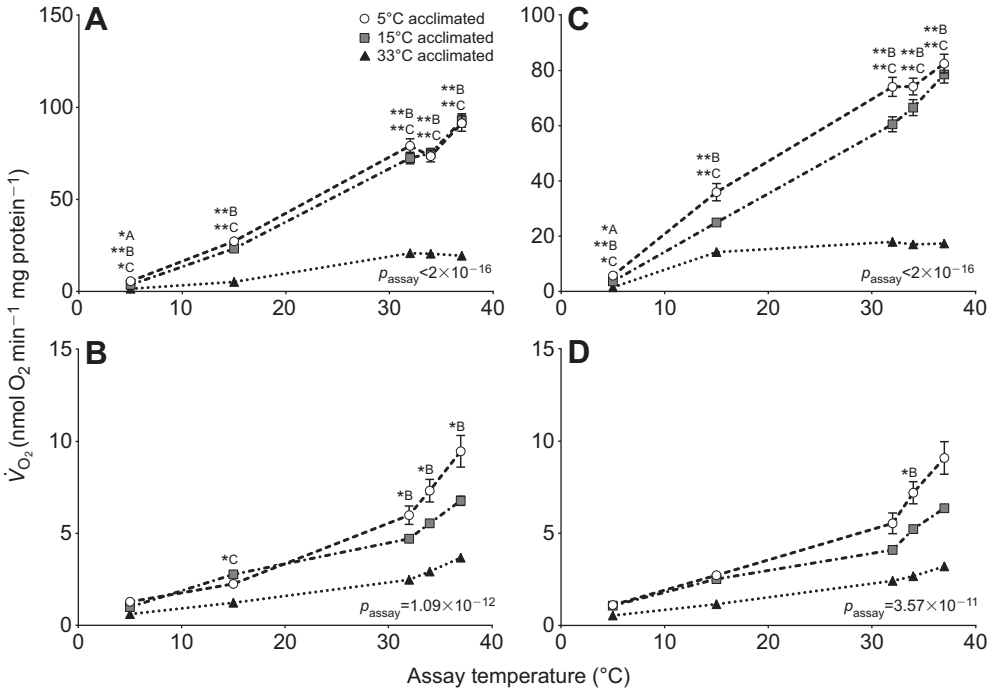

Fig. 2. Effects of acclimation and assay temperature on respiration rate of killifish mitochondria fueled with different complex I-linked substrates. Mitochondria from killifish acclimated to 5, 15 or 33°C were provided glutamate+malate (A,B) or pyruvate+malate (C,D), which enter the Krebs cycle via different pathways. Respiration rate was measured under state 3 (A,C) or state 4 (B,D) conditions. Assay temperature effects are indicated by *P*-value within each panel. Letters above each assay temperature indicate a significant difference between acclimations within an assay temperature (A, 5°C≠15°C; B, 5°C≠33°C; C, 15°C≠33°C). Asterisks denote the *P*-value of each acclimation effect (**P*<0.05, ***P*<0.01). Data are means±s.e.m. (*N*=5–6).

Increased assay temperature significantly increased state 3 respiration rates fuelled with both glutamate+malate (Fig. 2A; linear mixed-effect model, P_{assay}<0.0001) and pyruvate+malate (Fig. 2C; linear mixed-effect model, P_{assay}<0.0001). Acclimation effects on respiration fuelled by glutamate+malate (linear mixed-effect model, $P_{acclimation}$<0.0001) and pyruvate+malate (linear mixed-effect model, $P_{acclimation}$<0.0001) were identical, such that acclimation to 33°C resulted in lower respiration rates (for all T_{assay}) compared with both 5 and 15°C groups. These lower temperature acclimation groups did not differ from each other, except at T_{assay}=5°C. Significant interaction effects between acclimation and assay temperature on state 3 respiration were detected for both glutamate+malate (linear mixed-effect model, $P_{interaction}$<0.0001) and pyruvate+malate (linear mixed-effect model, $P_{interaction}$<0.0001).

State 4 (leak) respiration fuelled by glutamate+malate (Fig. 2B) and pyruvate+malate (Fig. 2D) also behaved similarly. Leak respiration rates fuelled by glutamate+malate (linear mixed-effect model, P_{assay}<0.0001) and pyruvate malate (linear mixed-effect model, P_{assay}<0.0001) increased with increasing T_{assay}. Significant acclimation effects were detected for both glutamate+malate (linear mixed-effect model, $P_{acclimation}$<0.0001) and pyruvate+malate (linear mixed-effect model, $P_{acclimation}$<0.0001). No significant interaction effects were detected. *Post hoc* analyses revealed that acclimation to 5°C increased leak respiration compared with 33°C for both substrates. Acclimation to 15°C increased leak respiration compared with 33°C; however, this only occurred at T_{assay}=15°C when fuelled with glutamate+malate.

Respiratory control ratio

We calculated RCRs to estimate changes in mitochondrial coupling following thermal acclimation and changes in assay temperature. RCR resulting from flux through ETS complex II (Fig. 3A) was significantly affected by assay temperature (linear mixed-effect model, P_{assay}<0.0001), with no significant effect of acclimation temperature. However, there was a significant interaction effect (linear mixed-effect model, $P_{interaction}$=0.0298), such that RCR was highest in the 5°C and 33°C acclimation groups assayed at their respective acclimation temperatures, although these differences were not detected in *post hoc* tests.

In contrast, RCR resulting from flux through ETS complex I exhibited an entirely different pattern. We detected a significant assay temperature effect for both glutamate+malate (Fig. 3B, linear mixed-effect model, P_{assay}<0.0001) and pyruvate+malate (Fig. 3C, linear mixed-effect model, P_{acute}<0.0001). In addition, glutamate+malate (linear mixed-effect model, $P_{acclimation}$<0.0001, $P_{interaction}$=0.0298) and pyruvate+malate (linear mixed-effect model, $P_{acclimation}$<0.0001, $P_{interaction}$=5.97×10^{-3}) RCRs were subject to significant acclimation and interaction effects. RCRs calculated from fish acclimated to 33°C were lower compared with other acclimation groups for the majority of assayed temperatures. This effect is driven by the lower state 3 respiration rates in this group. Differences in RCR between the 5 and 15°C acclimation groups were dependent on T_{assay}, such that 5°C acclimated fish exhibited higher RCRs at lower T_{assay} and 15°C acclimated fish surpassed the 5°C group at higher T_{assay}.

Proton leak kinetics

We measured the kinetics of proton leak over varying membrane potentials in order to provide insight into the maintenance of Δp under conditions considered to be more physiologically relevant (compared with rates at $\Delta\Psi_{m,max}$ measured previously). To compare across acclimation temperatures, proton leak kinetics were analyzed for each mitochondrial preparation and the kinetic parameter k (the rate constant) was extracted. Regardless of assay temperature, no significant differences in k across acclimation groups were detected (Fig. 4A, T_{assay}=5°C, one-way ANOVA, $P_{acclimation}$=0.742, $k_{5°C}$=0.0044±5.6×10^{-3}, $k_{15°C}$=0.0156±8.1×10^{-3}, $k_{33°C}$=0.0069±1.36×10^{-3}; Fig. 4B, T_{assay}=15°C, one-way ANOVA, $P_{acclimation}$=0.723, $k_{5°C}$=0.0401±1.59×10^{-2}, $k_{15°C}$=0.0227±6.2×10^{-3}, $k_{33°C}$=0.0375±2.45×10^{-2}; Fig. 4C, T_{assay}=33°C, one-way ANOVA, $P_{acclimation}$=0.774, $k_{5°C}$=0.0638±1.41×10^{-2}, $k_{15°C}$=0.0570±1.11×10^{-2}, $k_{33°C}$=0.0498±1.55×10^{-2}).

The Journal of Experimental Biology (2015) 218, 1621-1631 doi:10.1242/jeb.120444

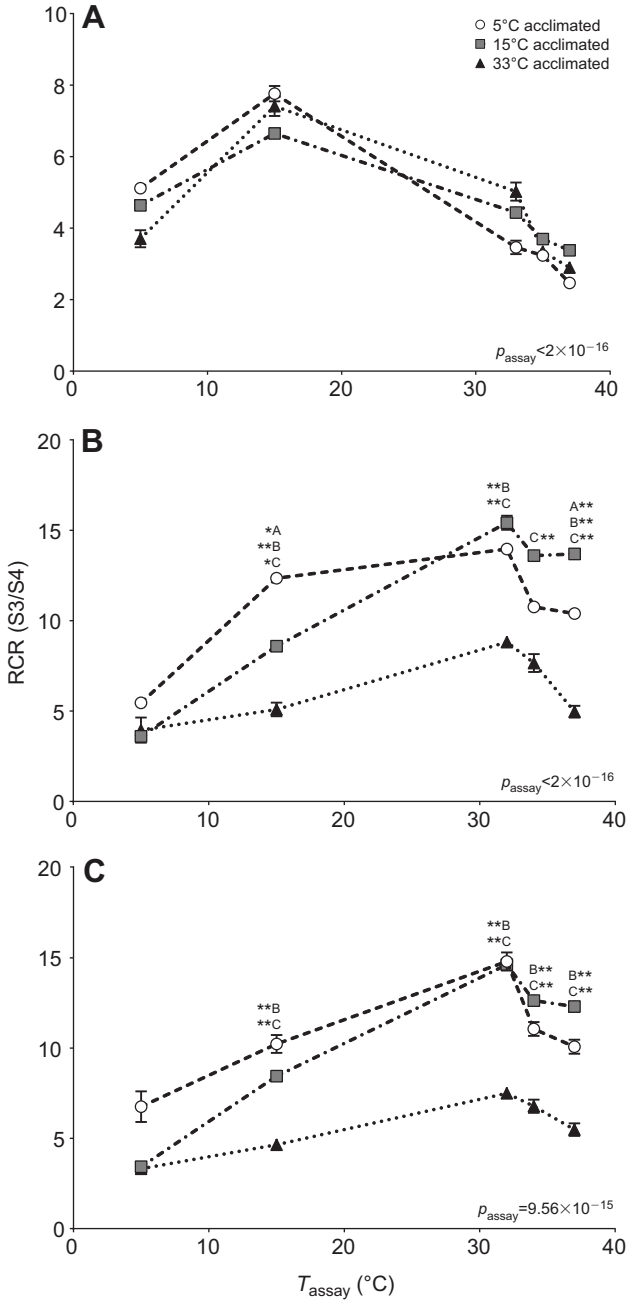

Fig. 3. Effects of acclimation and assay temperature on the respiratory control ratio (the ratio of state 3 and 4 respiration) of killifish mitochondria. Mitochondria were provided succinate (A), glutamate+malate (B) or pyruvate+malate (C). Assay temperature effects are indicated by *P*-value within each panel. Letters above each assay temperature indicate a significant difference between acclimations within an assay temperature (A, 5°C≠15°C; B, 5°C≠33°C; C, 15°C≠33°C). Asterisks indicate the *P*-value of each acclimation effect (*P<0.05, **P<0.01). Data are means±s.e.m. (N=7–9).

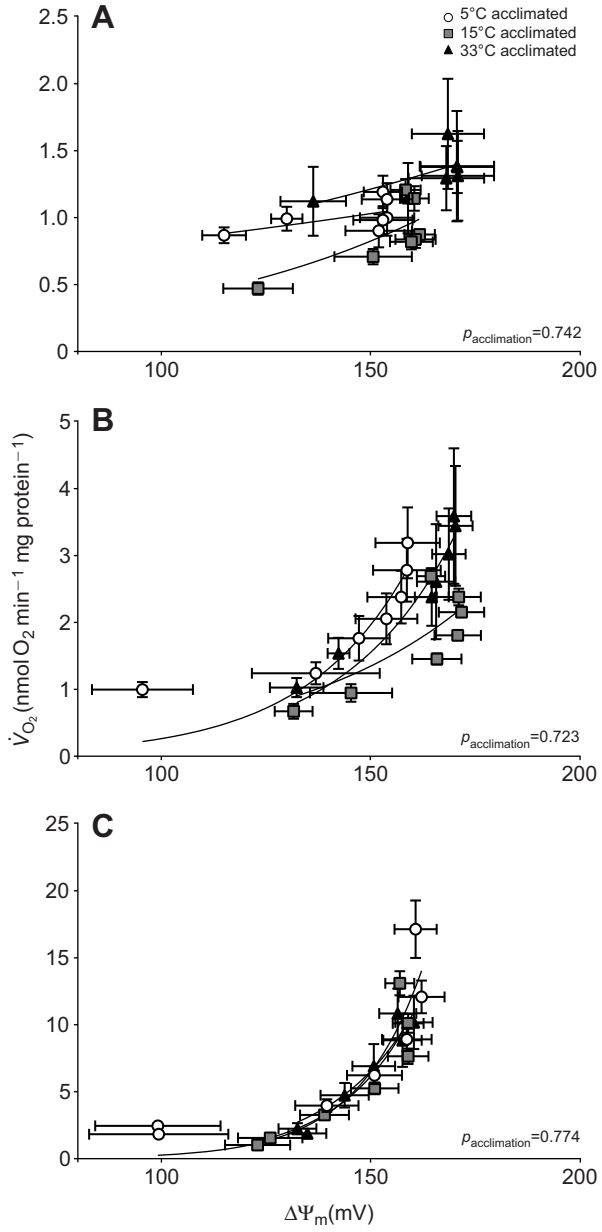

Fig. 4. Killifish liver mitochondrial proton leak kinetics assayed over a range of temperatures following acclimation to 5, 15 or 33°C. Proton leak assayed at 5°C (A), 15°C (B) and 33°C (C). Kinetics were measured by titrating saturating state 4 respiration (with succinate as the substrate) with additions of malonate (seven additions). *P*-values for comparisons among acclimation groups of equation parameters (*k*) are indicated in each panel. Data are means±s.e.m. (N=7–9).

Reactive oxygen species production

We estimated mitochondrial ROS production rate as H_2O_2 production ($\dot{V}_{H_2O_2}$) in order to assess deleterious extra-mitochondrial effects resulting from changes in proton leak. Basal and maximum ROS production rates behaved similarly, and increases in assay temperature significantly increased production for all acclimation groups (Fig. 5A, B, linear mixed-effect model, $P_{acute,\ basal}$<0.0001, $P_{acute,\ max}$<0.0001). No significant interaction or acclimation effects were detected. Free radical leak (FRL; $\dot{V}_{H_2O_2}$ corrected for mitochondrial oxygen consumption) was also affected by acute assay temperature (Fig. 5C, linear mixed-effect model, P_{acute}=5.97×10^{-3}), with a trend towards increased FRL at 5°C, although this was not detected by *post hoc* tests. No significant interaction or acclimation effects on FRL were detected.

DISCUSSION

In this study, we assessed the mechanisms and costs of mitochondrial thermal acclimation in the eurythermal Atlantic killifish *F. heteroclitus*. Low-temperature acclimation resulted in a modest compensation of respiration that was not specific to any one ETS complex. In contrast, high-temperature acclimation induced a large

The Journal of Experimental Biology (2015) 218, 1621-1631 doi:10.1242/jeb.120444

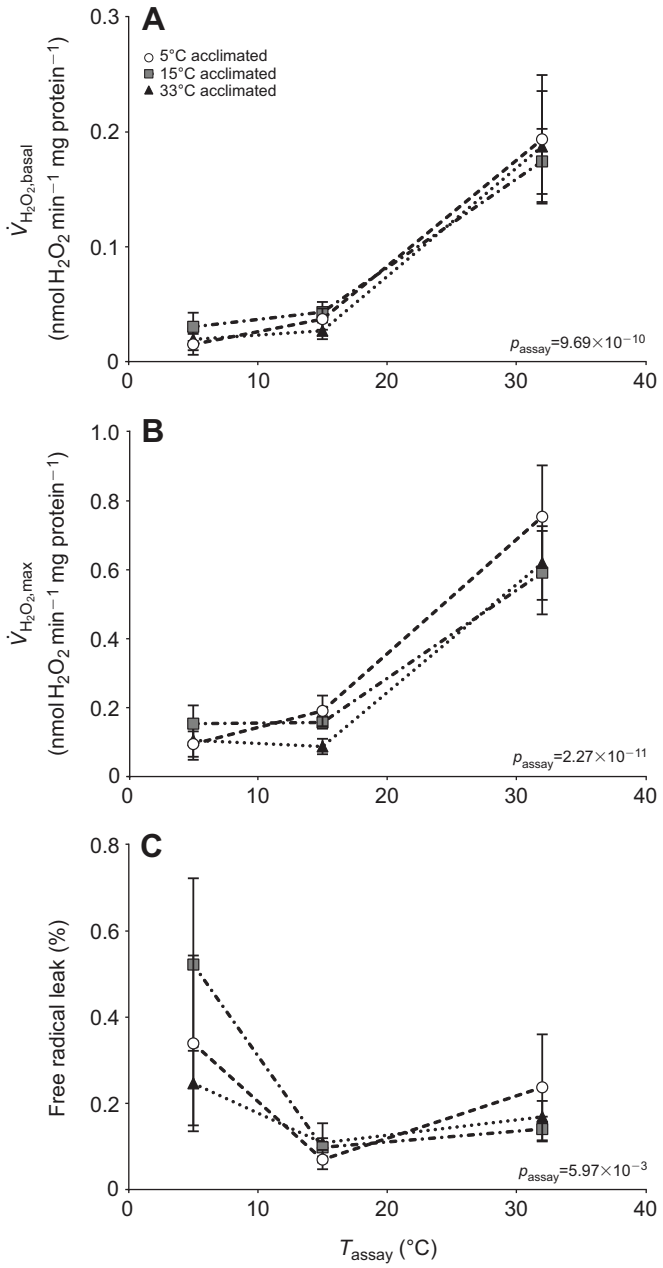

Fig. 5. Liver mitochondrial H_2O_2 (i.e. reactive oxygen species) production rate and free radical leak of killifish following thermal acclimation. Basal $\dot{V}_{H_2O_2}$ (A), maximum $\dot{V}_{H_2O_2}$ (B) and free radical leak (C). Assay temperature effects are indicated by *P*-value within each panel. Data are means±s.e.m. (*N*=7–9).

suppression of respiration, which was associated almost exclusively with substrates that supply electrons to ETS complex I. Of particular interest was our finding that these large changes in mitochondrial function occurred without a loss of $\Delta\Psi_m$ or increased extra-mitochondrial ROS production, despite the fact that low-temperature acclimation resulted in greater declines in RCR at high temperatures and high-temperature acclimation resulted in declines in RCR at low temperature relative to the other acclimation groups.

Modest compensation following low-temperature acclimation

Low-temperature compensation of mitochondrial respiration has been demonstrated in several ectothermic species (Dos Santos et al., 2013; Kraffe et al., 2007; Fangue et al., 2009). These increases in functional capacity are thought to play a role in maintaining ATP homeostasis (reviewed by O'Brien, 2011). We observe similar effects, but the magnitude of compensation between *F. heteroclitus* acclimated to 5 and 15°C is small compared with patterns in other species, and respiration only differed significantly at low assay temperatures (Fig. 1A–C and Fig. 2). For example, Q_{10} calculated from 5°C acclimation fish between T_{assay}=5 and 15°C was 4.46 for pyruvate+malate-fuelled state 3 respiration (Fig. 2C) but 3.66 when compared between 5 and 15°C acclimated fish assayed at their respective acclimation temperatures, demonstrating a Precht type III (i.e. partial) compensation of respiration (Precht, 1958). These data are in agreement with previous observations of killifish liver mitochondrial respiration, demonstrating a limited low-temperature acclimation response (Fangue et al., 2009).

The relatively limited cold-compensation of respiration that we observed in *F. heteroclitus* compared with patterns in other species (St.-Pierre et al., 1998) suggests that the wide thermal breadth and substantial plasticity in the whole-organism thermal tolerance of *F. heteroclitus* is not associated with exceptional plasticity in mitochondrial function. It is important to note, however, that the apparent discrepancy between our results and previous studies in other eurythermal species such as goldfish (Dos Santos et al., 2013) may be driven by experimental design. For example, if we had compared mitochondrial respiration only between our two extreme acclimation groups (i.e. 5 and 33°C) we would have concluded that there is a large cold-compensation effect, similar to that observed in other studies (e.g. Dos Santos et al., 2013). Indeed, studies of mitochondrial thermal acclimation often utilize a two-point (low versus high temperature) comparison. This design, however, has the potential to confound interpretation of the low-temperature acclimation response, if there is a suppressive effect of warm acclimation. While we do not discount the compensatory changes observed in previous studies of cold acclimation, caution in interpreting the magnitude of these effects is warranted. As a consequence, we recommend including intermediate acclimation treatments in order to avoid these potentially confounding effects.

Our observation of modest low-temperature acclimation effects on mitochondrial respiration compared with mitochondria from fish acclimated at intermediate temperatures indicates that if maintenance of ATP balance is to be achieved, mechanisms other than increases in functional capacity (on a per mitochondrion protein basis) must be recruited. Altering mitochondrial structure and quantity can increase capacity in tandem with changes in mitochondrial biochemical function (Guderley and St-Pierre, 2002). Potential mechanisms might include increases in mitochondrial volume density and cristae surface area. Indeed, these changes have been demonstrated in killifish following low-temperature acclimation (Dhillon and Schulte, 2011). Together, our results demonstrate that increases in mitochondrial function following low-temperature acclimation do occur; however, the contribution of these changes to maintaining ATP balance may be small in comparison to changes in mitochondrial quantity and structure. Alternatively, at low temperatures, *F. heteroclitus* may exploit a strategy of only partial compensation, taking advantage of the metabolic suppression caused by low temperatures to reduce metabolic demand in the winter when food resources could be limited. This hypothesis is consistent with the observed suppression of whole-organism metabolic rates in response to cold acclimation in this species (Healy and Schulte, 2012).

The Journal of Experimental Biology (2015) 218, 1621-1631 doi:10.1242/jeb.120444

Suppression of mitochondrial respiration during warm acclimation

Although we observed modest low-temperature compensation of mitochondrial respiration, high-temperature acclimation (33°C) resulted in a clear reduction of mitochondrial function (Figs 1 and 2). This response was not observed when killifish were acclimated to 25°C (Fangue et al., 2009). At the whole-animal level, acclimation to 25 and 33°C induces different responses, and aerobic scope is maintained only at the lower of these temperatures (Healy and Schulte, 2012). This suggests that acclimation to 33°C is stressful for killifish. Indeed, chronic exposure to a marginally higher ambient temperature (T_a=36.4°C) has been shown to induce mortality in killifish, with a significant loss of total muscle lipids and liver glycogen occurring at $T_{acclimation}$=29°C (Fangue et al., 2006, 2008). Our data demonstrating reductions in whole animal and liver mass following high-temperature acclimation supports this conclusion. Given that 33°C acclimated fish exhibit these changes while still being fed to satiation may be indicative of entrance into a state of negative energy balance or induction of hypometabolism.

The suppression of mitochondrial capacity we observed occurred with substrates that supply electrons to ETS complex I (Figs 1 and 2). Low rates of respiration through complex I were observed with both of the substrates provided (i.e. pyruvate+malate or glutamate +malate; Fig. 2), indicating that transport and decarboxylation of pyruvate (by pyruvate dehydrogenase) are not major points of modification. This observation is similar to the acute low-temperature response in the rainbow trout (Blier and Guderley, 1993). This suggests a possible reduction in total oxidative phosphorylation capacity following high-temperature acclimation. Indeed, complex I and complex II raw oxygen consumption rates and $\Delta\Psi_m$ do not differ greatly (Fig. 1A,B; T_{assay}=15°C), suggesting a fairly equal contribution to total mitochondrial flux. As a large multi-subunit protein complex that contributes heavily to mitochondrial Δp, complex I is a logical candidate for modification during thermal acclimation (Efremov et al., 2010). Indeed, differences in complex I activity have been suggested to play a role in adaptive differences in thermal tolerance among killifish species and sub-populations (Loftus and Crawford, 2013). Alternatively, it is possible that modifications in the activity of one or more tricarboxylic acid cycle enzymes (although not of succinate dehydrogenase) could account for these observations.

Our observation of decreased mitochondrial flux following high-temperature acclimation may be a consequence of entrance into a state of negative energy balance, which may induce hypometabolism. At the whole-animal level, acclimation to high temperatures induces a slight reduction in routine metabolism in killifish, which may be indicative of suppressed metabolism (Healy and Schulte, 2012). Hypometabolism induced by fasting and short photophase in *Mus musculus* and *Phodopus sungorus* suppresses complex I-linked but not complex II-linked mitochondrial respiration (Brown and Staples, 2011). A similar observation has been made in liver mitochondria from fasted CD1 mice and is thought to occur because of a reduction in supercomplexing between complexes I and III, and increased fatty acid oxidation (Lapuente-Brun et al., 2013). Similarly, the observed alterations in the contribution of complex I to total ETS flux in killifish may occur as a result of increased utilization of lipid stores, as demonstrated in fasted *Oncorhynchus mykiss* (Morash and McClelland, 2011). Collectively, our data reveal mitochondrial mechanisms that may be used to alleviate high-temperature-induced mismatches between whole-animal metabolic demand and consumption (Lemoine and Burkepile, 2012; Iles, 2014).

Thermal acclimation does not result in large dysfunction of coupling, Δp or ROS production

To investigate whether acclimation-induced changes in respiration were associated with mitochondrial dysfunction (e.g. uncoupling), we compared RCR (the ratio of mitochondrial ADP-phosphorylating respiration to leak respiration) among acclimation treatments (Fig. 3). We observed a decrease in RCR for all acclimation treatments at high assay temperatures (Fig. 3). Reductions in mitochondrial function at high temperatures have been proposed to limit whole-animal thermal tolerance. Indeed, a reduction in cardiac mitochondrial ATP-synthesizing capacity is known to occur at temperatures just below those that induce heart failure in *Notolabrus celidotus* (Iftikar and Hickey, 2013).

When RCR was calculated with respiration fueled through complex II, it declined more sharply when assayed at 5°C in the 33°C acclimated fish compared with other acclimation groups (Fig. 3A). Conversely, RCR from 5°C acclimated fish decreased marginally at high T_{assay}. As a result, a higher RCR was observed with 5°C and 33°C acclimated fish at their respective assay temperatures, which may be indicative of beneficial acclimation. However, these differences were small and were not detected in *post hoc* analyses. When fuelled through complex I (Fig. 3B,C), RCR for 33°C acclimated fish was lower than that of the other acclimation groups. Although low RCR is often interpreted as increased uncoupling, the lower RCR in 33°C acclimated fish is driven primarily by suppression of ADP-phosphorylating respiration (state 3; Fig. 2A,C) and not increased leak respiration (state 4; Fig. 2B,D), emphasizing an important caveat of interpreting RCR discussed by Gnaiger (2012).

Changes in inner mitochondrial membrane (IMM) lipid composition and mitochondrial enzyme activities during thermal acclimation are thought to cause mitochondrial dysfunction during acute thermal shifts: a mechanism proposed to cause shifts in thermal optima (Guderley, 2004). We assessed state 4 (i.e. leak) respiration and ability to maintain $\Delta\Psi_m$ as metrics of these costs. In principle, significant reductions in $\Delta\Psi_m$ would reflect a pathological loss of Δp, whereas high $\Delta\Psi_m$ would be a consequence of uncontrolled generation of Δp. We observed a consistent pattern of increased leak respiration in 5°C acclimated fish at high T_{assay} (Figs 1C and 2B,D); however, $\Delta\Psi_m$ does not decline under these conditions (Fig. 1F). Under maximum state 3 conditions (ETS complex I- and complex II-linked, Fig. 1D,E), $\Delta\Psi_m$ did not differ among acclimation treatments. The observation that $\Delta\Psi_m$ is sustained, particularly given the large changes in complex I-linked ETS flux, may demonstrate that the suppression of respiration is regulated and does not incur a cost in terms of function. In contrast to state 3 flux, $\Delta\Psi_m$ fuelled under state 4 conditions (complex II-linked) was lower in 33°C acclimated fish, but only at high assay temperatures (T_{assay}=35°C and 37°C, Fig. 1F). We initially predicted that acute increases in temperature would cause a decline in $\Delta\Psi_m$ in low-temperature acclimated fish because of a loss of coupling. Our results are contrary to our initial prediction and are difficult to account for, especially given that RCR and state 4 respiration (complex II-linked) in 33°C acclimated fish do not differ from those at other acclimation temperatures (Figs 1C and 3A). This decline in $\Delta\Psi_m$ may be indicative of the onset of pathological function, but given that RCR and state 4 respiration are nonetheless sustained at this temperature, we would predict only limited loss of function.

Acute increases to high temperatures decreased maximum $\Delta\Psi_m$ under state 3 conditions for all acclimation treatments (Fig. 1D,E). This decline in $\Delta\Psi_m$ may be a result of increased mitochondrial uncoupling. Given that RCRs also declined at high T_{assay}, some

The Journal of Experimental Biology (2015) 218, 1621-1631 doi:10.1242/jeb.120444

level of mitochondrial uncoupling is likely to occur (Fig. 3). Although it appears that high T_{assay} does have an effect on mitochondrial coupling, these responses are at best only slightly modulated by thermal acclimation. Furthermore, $\Delta\Psi_m$ under maximum state 3 conditions (Fig. 1D) did not differ among acclimation groups assessed with complex I-linked fuels, indicating that if our observed declines in RCR were a result of increased uncoupling they do not cause a dysfunction in maintaining Δp. As a result, killifish seem to be able to maintain coupling across acclimation treatments, but are still subject to loss of coupling following acute increases in T_{assay}.

To ensure that our observation of limited thermal acclimation effects on $\Delta\Psi_m$ sensitivity was not an artifact of having measured ETS flux under saturating conditions, we measured leak ETS flux over a range of mV (proton leak kinetics; titrated state 4 respiration and $\Delta\Psi_m$ measured in tandem) through complex II (Fig. 4) and observed no acclimation effect. This contrasts with the warm-acclimation response in lugworms (*Arenicola marina*), which respond with an increase in $\Delta\Psi_m$ (Keller et al., 2004). However, the warm-acclimated lugworms were also in spawning, which makes it difficult to disentangle life-history and thermal effects. Altogether, our data are unique in that they are among the few direct assessments of thermal acclimation effects on $\Delta\Psi_m$ and they clearly demonstrate the ability of *F. heteroclitus* to maintain $\Delta\Psi_m$ over a wide thermal range in spite of the profound changes in mitochondrial ETS flux (particularly during warm acclimation).

We predicted increased ROS production as a consequence of low-temperature acclimation, as it is thought to be associated with pathological ETS flux during acute thermal shifts to high temperatures (Guderley, 2004). Similar to our observations of $\Delta\Psi_m$, ROS production rate and free radical leak through ETS complex II did not differ among acclimation treatments (Fig. 5A,B). Indeed, increases in assay temperature increased ROS production for all acclimation groups, emphasizing the potentially stressful effects of high ambient temperature. Although we did not observe a significant effect of acclimation on ROS production, it is important to acknowledge potential limitations of our methodology. By estimating ROS production as extra-mitochondrial [H_2O_2] we were unable to detect endo-mitochondrial ROS, because these may be scavenged within the mitochondrion prior to detection. Nonetheless, our measurements are informative for estimating the potential for cytosolic damage. Indeed, our observation of no change in ROS production is reflected in the fact that thermal acclimation has little effect on lipid peroxidation rate and antioxidant enzyme activities in killifish (Grim et al., 2010). Because we measured ROS production as a result of succinate-fueled state 4 respiration (which drives ROS production primarily through complex III), we largely bypassed complex I, which can be an important contributor to ROS production *in vivo* (Turrens and Boveris, 1980). Given the causative link between increases in state 4 respiration and ROS production, and our observed trends of decreased complex I-linked state 4 respiration in 33°C acclimated fish (Fig. 2B,D), we might predict decreased ROS production in this group. Nonetheless, complex III has been shown to produce greater amounts of ROS compared with complex I under similar assay conditions, and so our observations have physiological importance (Chen et al., 2003).

Similar to our measurements of ROS production, free radical leak (ROS production adjusted to mitochondrial O_2 consumption) did not differ among acclimation treatments (Fig. 5C). Although a trend of increased FRL at low assay temperatures was observed (with a minimal effect size), this is likely to be driven by low respiration rates rather than actual increases in ROS production. These data therefore provide additional support to our conclusion that mitochondrial thermal acclimation does not result in large trade-offs in mitochondrial function in killifish.

Conclusions

This study provides a comprehensive assessment of the mechanisms and costs associated with mitochondrial thermal acclimation in a eurythermal teleost. Our data clearly demonstrate the wide range over which killifish can modify mitochondrial activity in response to thermal acclimation. A novel finding is that these changes were largely associated with suppression of ETS flux through complex I following acclimation to high temperatures and not flux through complex II or pyruvate dehydrogenase (PDH). We propose that these shifts in ETS flux may occur in part, as a result of entrance into a state of negative energy balance at high temperatures. We predicted that changes in mitochondrial function following thermal acclimation would induce a loss of function during acute thermal shifts, perhaps accounting for changes in whole-animal thermal tolerance. Our metrics of dysfunction (loss of Δp, increased ROS production) remained largely unaffected by acute thermal shifts, although we observed modest effects on RCR. Thus these data provide only limited support for a direct link between mitochondrial plasticity and plasticity in whole-animal thermal tolerance. Instead, our data demonstrate that killifish have a profound ability to maintain mitochondrial function across large acute shifts in temperature and may suggest a mechanism underlying the eurythermal physiology of this species. Further investigations into the thermal acclimation response of complex I, through studies on pre and post-translational modifications as well as mechanistic responses (e.g. IMM modification, kinetics of ETS flux), especially in the heart, will prove invaluable to improving understanding of physiological responses to changes in environmental temperature.

MATERIALS AND METHODS

Reagents

All reagents were obtained from Sigma-Aldrich (Oakville, ON).

Animals

Treatment of animals was completed in accordance with the University of British Columbia animal care protocol #A01-0180. Adult northern killifish (*Fundulus heteroclitus macrolepidotus* Walbaum 1792) were collected in Odgen's Pond estuary, Jimtown, NS (45°71′N; −61°90′W) during September of 2013. Fish were housed at the University of British Columbia Aquatics Facility in 190 litre tanks with biological filtration at T_a=20±2°C, 20 ppt salinity, and 12 h:12 h L:D photoperiod for 4 weeks prior to experimental acclimation. Food (Tetrafin Max; Rolf C. Hagen Inc., Montreal, QC) was provided once daily to satiation. Following the holding period, fish were randomly distributed into 114 litre acclimation tanks with T_a=5, 15 or 33°C and 12 h:12 h L:D photoperiod for 4 weeks prior to sampling. We chose a high acclimation temperature of 33°C as opposed to 30°C because of the induction of breeding physiology at 30°C. Trends of increased gonadosomatic index and spermatogenesis have been noted in the killifish following acclimation to temperatures ranging from 20 to 25°C (Healy and Schulte, 2012; Matthews, 1939). Acclimation to 33°C induces a warm-acclimation response while avoiding these artifacts.

Isolation of liver mitochondria

Seven randomly selected killifish were pooled for each mitochondrial sample. Killifish were killed (08:00 h PST) by cervical dislocation; liver tissue (approximately 1 g total tissue) was excised and finely minced (1 mm^3 pieces) in ice-cold homogenization buffer (250 mmol l^{-1} sucrose, 50 mmol l^{-1} KCl, 0.5 mmol l^{-1} EGTA, 25 mmol l^{-1} KH_2PO_4, 10 mmol l^{-1} HEPES, 1.5% BSA, pH=7.4 at 20°C). Liver pieces were homogenized using five passes of a loose-fitting Teflon pestle and filtered through 1-ply

The Journal of Experimental Biology (2015) 218, 1621-1631 doi:10.1242/jeb.120444

cheesecloth. Homogenate was centrifuged at 600 ***g*** at 4°C for 10 min. The fat layer was aspirated from the supernatant and filtered through 4-ply cheesecloth. Defatted supernatant was centrifuged at 6000 ***g*** for 10 min at 4°C. The pellet was isolated, washed twice in homogenization buffer and resuspended in 800 µl homogenization buffer (approximately 11 mg ml^{-1} protein). Mitochondria were kept on ice and used to measure respiration, membrane potential, proton leak kinetics and ROS production. Protein content was determined by the Bradford (1976) method with BSA standards.

Mitochondrial respiration rate and proton motive force

Mitochondrial respiration rate ($\dot{V}_{O_2}$) and proton motive force (Δp; estimated as mitochondrial membrane potential, $\Delta\Psi_m$) measurements were completed using a high-resolution respirometry system (O2k MiPNetAnalyzer) and tetraphenylphosphonium (TPP^+) selective electrodes (Oroboros Instruments; Innsbruck, Austria). Oxygen electrodes were calibrated at each assay temperature (T_{assay}=5, 15, 33, 35, and 37°C) with air-saturated, and oxygen-depleted (achieved with a yeast suspension) MiRO5 assay buffer (110 mmol l^{-1} sucrose, 0.5 mmol l^{-1} EGTA, 3 mmol l^{-1} $MgCl_2$, 60 mmol l^{-1} K-lactobionate, 20 mmol l^{-1} taurine, 10 mmol l^{-1} KH_2PO_4, 20 mmol l^{-1} HEPES, 1% BSA, pH=7.1 at 30°C; Gnaiger and Kuznetsov, 2002) using O_2 solubilities published by Gniager and Forstner (1983).

Measurement of $\Delta\Psi_m$ and $\dot{V}_{O_2}$ through ETS complex I, and complex II were completed using methodologies modified from Brand (1995). Through preliminary experiments we determined that incubation of mitochondrial preparations with nigericin (80 ng ml^{-1}; which eliminates the ΔpH component of Δp, leaving only $\Delta\Psi_m$) had a large inhibitory effect on mitochondrial respiration. Given that $\Delta\Psi_m$ is the major contributor to mitochondrial Δp (discussed by Nicholls and Ferguson, 2013; Brown et al., 2007), we decided to not use nigericin and approximated Δp using $\Delta\Psi_m$. Following air equilibration of 2 ml MiRO5 assay buffer to T_{assay}=5, 15, 33, 35, or 37°C, TPP^+-selective electrodes were introduced to the chamber and calibrated with five additions of TPP^+ (the first 1 µmol l^{-1} TPP^+ addition was followed by four additions of 0.5 µmol l^{-1} TPP^+, 3 µmol l^{-1} TPP^+ total). Liver mitochondrial protein (0.5 mg) was added to the chamber followed by ADP (1 mmol l^{-1}). Flux through complex I was obtained through introduction of glutamate (10 mmol l^{-1}) and malate (2 mmol l^{-1}). Once state 3 (ADP-phosphorylating) and membrane potential measurements were obtained, flux through complex I was inhibited with rotentone (0.5 µmol l^{-1} in ethanol). Complex II was activated with the addition of succinate (10 mmol l^{-1}). State 4 (ADP non-phosphorylating) respiration rates and membrane potential were approximated through inhibition of the ATP synthase with oligomycin (2 µg ml^{-1} dissolved in ethanol). Carbonyl cyanide-*p*-trifluoro-methoxyphenylhydrazone (FCCP 1 µmol l^{-1}, dissolved in ethanol) was added to uncouple the mitochondria and assess electrode drift. TPP^+ dilution and substrate-inhibitor effects on TPP^+ measurements were corrected by measuring TPP^+ concentration during a substrate-inhibitor protocol in the absence of mitochondria. RCR (the ratio of state 3 and state 4 respiration rates) was calculated as a means of estimating mitochondrial coupling.

External TPP^+ concentrations were used to calculate $\Delta\Psi_m$ using a modified Nernst equation (Rottenberg, 1984).

$$\Delta\Psi_m = a \log\left(\frac{([TPP^+]_{total}/[TPP^+]_{free}) - v_{external} - K'_o \text{ mg protein}}{v_{mt} \text{ mg protein} + K'_i \text{ mg protein}}\right) \quad (1)$$

In Eqn 1, a is the temperature-dependent coefficient ($a=RT/zF$, where R is the universal gas constant, T is the absolute temperature, z is the ion's valence and F is the Faraday constant), $v_{external}$ is the volume outside the mitochondria, K'_i, and K'_o are partition coefficients used to correct for nonspecific internal and external binding of TPP^+, respectively, and v_{mt} is the mitochondrial matrix volume. Values for K' (Rottenberg, 1984) and v_{mt} (Halestrap, 1989) were set according to literature values from rat liver mitochondria.

Although matrix volume has the potential to vary with temperature, changes in this parameter result in negligible changes in membrane potential in the presence of TPP^+ (Rottenberg, 1984). We calculate that a 50% increase in v_{mt} results in a 1% change in the estimated membrane potential of killifish mitochondria. Non-specific TPP^+ binding to dipalmitoylphosphatidylcholine liposomes has been shown to be temperature sensitive (Demura et al., 1987). The effect this has on isolated mitochondria is unknown, and while changes in K' have a larger effect on calculated values of membrane potential when compared with an equivalent change of v_{mt} (5% vs 1%, respectively), this is within our accepted range of error. We therefore assumed that nonspecific binding of TPP^+ and matrix volume remained constant across our manipulations. This assumption does not affect the analysis of differences in $\Delta\Psi_m$ following thermal acclimation because mitochondria from all acclimation groups were assayed across the same range of temperatures.

Glutamate+malate and pyruvate+malate fuelled state 3 and 4 respiration rate

We assessed the effect of thermal acclimation on mitochondrial respiration rate (state 3 and state 4), in the absence of TPP^+ when fuelled by pyruvate+malate and glutamate+malate. Liver mitochondrial protein (0.3 mg) was added to 2 ml of air-saturated (T_{assay}=5, 15, 33, 35 or 37°C) MiRO5. This was followed by an addition of saturating ADP (1 mmol l^{-1}). State 3 respiration rates were obtained through the addition of glutamate (10 mmol l^{-1}) and malate (2 mmol l^{-1}), allowing for electron flux through complex I. State 4 respiration rates were approximated through the addition of oligomycin (2 µg ml^{-1} dissolved in ethanol). Pyruvate-fuelled state 3 and 4 respiration rates were obtained using the protocol described above with pyruvate (5 mmol l^{-1}) used in place of glutamate.

Proton leak kinetics

Proton leak kinetics were assessed using methods similar to those described above. Following air equilibration of 2 ml MiRO5 to T_{assay}=5, 15, 33, 35 or 37°C, and calibration of the TPP^+ electrodes, isolated liver mitochondria (0.5 mg) were added to the chamber. Rotenone (0.5 µmol l^{-1} in ethanol) and oligomycin (2 µg ml^{-1} dissolved in ethanol) were added to the chamber to inhibit flux through ETS complex I and the ATP synthase, respectively. State 4 respiration was approximated by measuring state 2 respiration in the presence of succinate (10 mmol l^{-1}). State 2 respiration was subsequently titrated with seven additions of malonate (0.5 mmol l^{-1} each). After the final titration step, mitochondria were uncoupled with FCCP (1 µmol l^{-1}, dissolved in ethanol). Proton leak kinetic curves for each mitochondrial preparation were fit to a two-parameter exponential growth equation using GraphPad Prism 6 software (La Jolla, CA) and the kinetic parameter: k (the rate constant) was used for statistical analysis.

ROS production rates

We estimated mitochondrial ROS production rates by measuring extra-mitochondrial H_2O_2 concentrations using a modified Amplex UltraRed (Invitrogen; Burlington, ON) assay. Liver mitochondria (total of 0.3 mg of mitochondrial protein) were incubated in 2 ml MiRO5 held at T_{assay}=5, 15, or 33°C. Mitochondrial ROS production was measured under state 4 conditions (i.e. in the absence of ADP) with saturating substrate. Basal (succinate and rotenone, concentrations as described above) and maximum (basal treatment in the presence of antimycin A; 2.5 µmol l^{-1}, dissolved in ethanol) ROS production rates were corrected against background rates (no substrates or inhibitors). Reactions were completed on a 96-well plate using a one-to-one ratio of mitochondrial sample and Amplex UltraRed working solution (horseradish peroxidase, 1 U activity per well; Amplex UltraRed 100 µmol l^{-1}, in DMSO; and sodium citrate 50 mmol l^{-1}, pH=6.0 at 20°C). Standards were composed of diluted H_2O_2. Absorbance (λ=565 nm) was measured using a spectrophotometer (Spectramax 190; Molecular Devices; Sunnyvale, CA). Linear regions of ROS production rate curves (0–45 min, sampled every 5 min) were used for analyses. Free radical leak (FRL) was calculated using the equation described by Barja et al. (1994).

Statistical analyses

All data are presented as means±s.e.m., with α=0.05. Sample size for each acclimation group is presented in relevant figures (where N=the number of

pooled mitochondrial preparations from 7 fish each). Statistical analyses were completed using R software (v3.0.2). We tested the effect of assay and acclimation temperature on mitochondrial respiration rates, membrane potential, RCR, FRL and ROS production rates using linear mixed-effect models. When significant acclimation effects were detected, we performed a one-way ANOVA within assay temperature. We applied *P*-values adjusted for false discovery rate to one-way ANOVAs using the Benjamini–Hochberg method (Thissen et al., 2002). Measurements of FRL, which are expressed as a percentage, were arcsine transformed prior to statistical analyses to ensure normality. Whole-animal characteristics and the rate constants extracted from proton leak kinetic analyses were compared across acclimation treatments within each assay temperature, using one-way ANOVAs. *Post hoc* Tukey's HSD analyses were conducted following the detection of significant major effects.

Acknowledgements
Thanks to Dr William Marshall for assistance with sample collection.

Competing interests
The authors declare no competing or financial interests.

Author contributions
D.J.C. and P.M.S. contributed to conception, design, interpretation of this experiment and revision of the article. D.J.C. contributed to data collection and drafting of the article.

Funding
Funding was provided by a National Science and Engineering Research Council (NSERC) discovery grant to P.M.S. and an NSERC CGS-D to D.J.C.

References
Abele, D., Heise, K., Pörtner, H. O. and Puntarulo, S. (2002). Temperature-dependence of mitochondrial function and production of reactive oxygen species in the intertidal mud clam *Mya arenaria*. *J. Exp. Biol.* **205**, 1831-1841.
Angilletta, M. J. (2009). *Thermal Adaptation*. Oxford: Oxford University Press.
Barja, G., Cadenas, S., Rojas, C., Pérez-Campo, R. and López-Torres, M. (1994). Low mitochondrial free radical production per unit O2 consumption can explain the simultaneous presence of high longevity and high aerobic metabolic rate in birds. *Free Radic. Res.* **21**, 317-327.
Blier, P. U. and Guderley, H. (1993). Effects of pH and temperature on the kinetics of pyruvate oxidation by muscle mitochondria from rainbow trout (*Oncorhynchus mykiss*). *Physiol. Zool.* **66**, 474-489.
Bradford, M. M. (1976). A rapid and sensitive method for the quantitation of microgram quantities of protein utilizing the principle of protein-dye binding. *Anal. Biochem.* **72**, 248-254.
Brand, M. D. (1995). Measurement of mitochondrial proton motive force. In *Bioenergetics* (ed. G. C. Brown and C. E. Cooper), pp. 39-62. Oxford: Oxford University Press.
Brown, J. C. L. and Staples, J. F. (2011). Mitochondrial metabolic suppression in fasting and daily torpor: consequences for reactive oxygen species production. *Physiol. Biochem. Zool.* **84**, 467-480.
Brown, J. C. L., Gerson, A. R. and Staples, J. F. (2007). Mitochondrial metabolism during daily torpor in the dwarf Siberian hamster: role of active regulated changes and passive thermal effects. *Am. J. Physiol. Regul. Integr. Comp. Physiol.* **293**, R1833-R1845.
Chen, Q., Vazquez, E. J., Moghaddas, S., Hoppel, C. L. and Lesnefsky, E. J. (2003). Production of reactive oxygen species by mitochondria: central role of complex III. *J. Biol. Chem.* **278**, 36027-36031.
Demura, M., Kamo, N. and Kobatake, Y. (1987). Mitochondrial membrane potential estimated with the correction of probe binding. *Biochim. Biophys. Acta* **894**, 355-364.
Dhillon, R. S. and Schulte, P. M. (2011). Intraspecific variation in the thermal plasticity of mitochondria in killifish. *J. Exp. Biol.* **214**, 3639-3648.
Dos Santos, R. S., Galina, A. and Da-Silva, W. S. (2013). Cold acclimation increases mitochondrial oxidative capacity without inducing mitochondrial uncoupling in goldfish white skeletal muscle. *Biol. Open* **2**, 82-87.
Efremov, R. G., Baradaran, R. and Sazanov, L. A. (2010). The architecture of respiratory complex I. *Nature* **465**, 441-445.
Egginton, S. and Johnston, I. A. (1984). Effects of acclimation temperature on routine metabolism muscle mitrochondrial volume density and capillary supply in the elver (Anguilla anguilla L.). *J. Therm. Biol.* **9**, 165-170.
Eliason, E. J., Clark, T. D., Hague, M. J., Hanson, L. M., Gallagher, Z. S., Jeffries, K. M., Gale, M. K., Patterson, D. A., Hinch, S. G. and Farrell, A. P. (2011). Differences in thermal tolerance among sockeye salmon populations. *Science* **332**, 109-112.
Fangue, N. A., Hofmeister, M. and Schulte, P. M. (2006). Intraspecific variation in thermal tolerance and heat shock protein gene expression in common killifish, *Fundulus heteroclitus*. *J. Exp. Biol.* **209**, 2859-2872.
Fangue, N. A., Mandic, M., Richards, J. G. and Schulte, P. M. (2008). Swimming performance and energetics as a function of temperature in Killifish *Fundulus heteroclitus*. *Physiol. Biochem. Zool.* **81**, 389-401.
Fangue, N. A., Richards, J. G. and Schulte, P. M. (2009). Do mitochondrial properties explain intraspecific variation in thermal tolerance? *J. Exp. Biol.* **212**, 514-522.
Gnaiger, E. (2012). *Mitochondrial Pathways and Respiratory Control*. 3rd edn. Innsbruck: OROBOROS MiPNet.
Gnaiger, E. and Forstner, H. (1983). Calculation of equilibrium oxygen concentration. In *Polarographic Oxygen Sensors*, pp. 321-333. Berlin; Heidelberg: Springer Berlin Heidelberg.
Gnaiger, E. and Kuznetsov, A. V. (2002). Mitochondrial respiration at low levels of oxygen and cytochrome c. *Biochem. Soc. Trans.* **30**, 252-258.
Grim, J. M., Miles, D. R. B. and Crockett, E. L. (2010). Temperature acclimation alters oxidative capacities and composition of membrane lipids without influencing activities of enzymatic antioxidants or susceptibility to lipid peroxidation in fish muscle. *J. Exp. Biol.* **213**, 445-452.
Guderley, H. (2004). Metabolic responses to low temperature in fish muscle. *Biol. Rev.* **79**, 409-427.
Guderley, H. and Johnston, I. (1996). Plasticity of fish muscle mitochondria with thermal acclimation. *J. Exp. Biol.* **199**, 1311-1317.
Guderley, H. and St-Pierre, J. (2002). Going with the flow or life in the fast lane: contrasting mitochondrial responses to thermal change. *J. Exp. Biol.* **205**, 2237-2249.
Halestrap, A. P. (1989). The regulation of the matrix volume of mammalian mitochondria in vivo and in vitro and its role in the control of mitochondrial metabolism. *Biochim. Biophys. Acta* **973**, 355-382.
Halestrap, A. P. (2012). The mitochondrial pyruvate carrier: has it been unearthed at last? *Cell Metab.* **16**, 141-143.
Hazel, J. R. (1995). Thermal adaptation in biological membranes: is homeoviscous adaptation the explanation? *Annu. Rev. Physiol.* **57**, 19-42.
Healy, T. M. and Schulte, P. M. (2012). Thermal acclimation is not necessary to maintain a wide thermal breadth of aerobic scope in the common killifish (*Fundulus heteroclitus*). *Physiol. Biochem. Zool.* **85**, 107-119.
Hochachka, P. W. and Somero, G. N. (2002). *Biochemical Adaptation*. 1st edn. Oxford: Oxford University Press.
Iftikar, F. I. and Hickey, A. J. R. (2013). Do mitochondria limit hot fish hearts? understanding the role of mitochondrial function with heat stress in *Notolabrus celidotus*. *PLoS ONE* **8**, e64120.
Iles, A. C. (2014). Toward predicting community-level effects of climate: relative temperature scaling of metabolic and ingestion rates. *Ecology* **95**, 2657-2668.
Keller, M., Sommer, A. M., Pörtner, H. O. and Abele, D. (2004). Seasonality of energetic functioning and production of reactive oxygen species by lugworm (*Arenicola marina*) mitochondria exposed to acute temperature changes. *J. Exp. Biol.* **207**, 2529-2538.
Khan, J. R., Iftikar, F. I., Herbert, N. A., Gnaiger, E. and Hickey, A. J. R. (2014). Thermal plasticity of skeletal muscle mitochondrial activity and whole animal respiration in a common intertidal triplefin fish, *Forsterygion lapillum* (Family: Tripterygiidae). *J. Comp. Physiol. B* **184**, 991-1001.
Kraffe, E., Marty, Y. and Guderley, H. (2007). Changes in mitochondrial oxidative capacities during thermal acclimation of rainbow trout *Oncorhynchus mykiss*: roles of membrane proteins, phospholipids and their fatty acid compositions. *J. Exp. Biol.* **210**, 149-165.
Lapuente-Brun, E., Moreno-Loshuertos, R., Acin-Perez, R., Latorre-Pellicer, A., Colás, C., Balsa, E., Perales-Clemente, E., Quirós, P. M., Calvo, E., Rodriguez-Hernandez, M. A. et al. (2013). Supercomplex assembly determines electron flux in the mitochondrial electron transport chain. *Science* **340**, 1567-1570.
Lemoine, N. P. and Burkepile, D. E. (2012). Temperature-induced mismatches between consumption and metabolism reduce consumer fitness. *Ecology* **93**, 2483-2489.
Loftus, S. J. and Crawford, D. L. (2013). Interindividual variation in complex I activity in *Fundulus heteroclitus* along a steep thermocline. *Physiol. Biochem. Zool.* **86**, 82-91.
Matthews, S. A. (1939). The effects of light and temperature on the male sexual cycle in Fundulus. *Biol. Bull.* **77**, 92-95.
Morash, A. J. and McClelland, G. B. (2011). Regulation of carnitine palmitoyltransferase (CPT) I during fasting in rainbow trout (*Oncorhynchus mykiss*) promotes increased mitochondrial fatty acid oxidation. *Physiol. Biochem. Zool.* **84**, 625-633.
Nicholls, D. G. and Ferguson, S. J. (2013). *Bioenergetics 4*. 4th edn. London: Academic Press.
O'Brien, K. M. (2011). Mitochondrial biogenesis in cold-bodied fishes. *J. Exp. Biol.* **214**, 275-285.
Pörtner, H. (2001). Climate change and temperature-dependent biogeography: oxygen limitation of thermal tolerance in animals. *Naturwissenschaften* **88**, 137-146.

Pörtner, H. O. and Farrell, A. P. (2008). Ecology: physiology and climate change. *Science* **322**, 690-692.
Precht, H. (1958). Concepts of temperature adaptation of unchanging reaction systems of cold-blooded animals. In *Physiological Adaptation* (ed. C. L. Prosser), pp. 51-78. Washington, DC: American Physiological Society.
Rottenberg, H. (1984). Membrane potential and surface potential in mitochondria: uptake and binding of lipophilic cations. *J. Membr. Biol.* **81**, 127-138.
Schulte, P. M., Healy, T. M. and Fangue, N. A. (2011). Thermal performance curves, phenotypic plasticity, and the time scales of temperature exposure. *Integr. Comp. Biol.* **51**, 691-702.
St.-Pierre, J., Charest, P.-M. and Guderley, H. (1998). Relative contribution of quantitative and qualitative changes in mitochondria to metabolic compensation during seasonal acclimatisation of rainbow trout *Oncorhynchus mykiss*. *J. Exp. Biol.* **201**, 2961-2970.
Strobel, A., Graeve, M., Poertner, H. O. and Mark, F. C. (2013). Mitochondrial acclimation capacities to ocean warming and acidification are limited in the antarctic Nototheniid fish, *Notothenia rossii* and *Lepidonotothen squamifrons*. *PLoS ONE* **8**, e68865.
Thissen, D., Steinberg, L. and Kuang, D. (2002). Quick and easy implementation of the Benjamini-Hochberg procedure for controlling the false positive rate in multiple comparisons. *J. Educ. Behav. Stat.* **27**, 77-83.
Turrens, J. F. and Boveris, A. (1980). Generation of superoxide anion by the NADH dehydrogenase of bovine heart mitochondria. *Biochem. J.* **191**, 421-427.